AGU PUBLICATIONS

Geophysical Research Letters

RESEARCH LETTER
10.1002/2015GL064381

Key Points:
- AMO leads to the decadal change of ENSO asymmetry
- ENSO asymmetry by AMO is due to nonlineary nature of convection-SST
- Central-to-eastern Pacific warming associated AMO drives ENSO asymmetry

Supporting Information:
- Text S1 and Figure S1
- Figure S1

Correspondence to:
S.-I. An,
sian@yonsei.ac.kr

Citation:
Sung, M.-K., S.-I. An, B.-M. Kim, and J.-S. Kug (2015), Asymmetric impact of Atlantic Multidecadal Oscillation on El Niño and La Niña characteristics, *Geophys. Res. Lett.*, *42*, 4998–5004, doi:10.1002/2015GL064381.

Received 29 APR 2015
Accepted 3 JUN 2015
Accepted article online 5 JUN 2015
Published online 24 JUN 2015

Asymmetric impact of Atlantic Multidecadal Oscillation on El Niño and La Niña characteristics

Mi-Kyung Sung[1], Soon-Il An[2], Baek-Min Kim[1], and Jong-Seong Kug[3]

[1]Division of Polar Climate Change Research, Korea Polar Research Institute, Incheon, South Korea, [2]Department of Atmospheric Sciences, Yonsei University, Seoul, South Korea, [3]School of Environmental Science and Engineering, Pohang University of Science and Technology, Pohang, South Korea

Abstract The long-lasting cold surface conditions of North Atlantic, i.e., the negative phase of Atlantic Multidecadal Oscillation (AMO), can intensify the El Niño–Southern Oscillation through the enhanced air-sea coupling under the increased central-to-eastern tropical Pacific mean sea surface temperature. However, the impact of warmer mean sea surface temperature (SST) is more efficient in the intensifying El Niño than La Niña, because of the nature of the exponential growth of atmospheric convection to SST change. Moreover, the farther eastward shift of the atmospheric convection during the negative AMO leads to the stronger El Niño due to the longer delayed negative feedback by oceanic waves. Therefore, the AMO mainly influences the El Niño intensity rather than La Niña intensity.

1. Introduction

The Atlantic Multidecadal Oscillation (AMO) is one of the most dominant long-term climate variability phenomena in the Northern Atlantic sector [*Kerr*, 2000; *Schlesinger and Ramankutty*, 1994]. A positive AMO phase comprises overall warming over the northern Atlantic Ocean, and a negative AMO phase has the opposite characteristic [*Enfield et al.*, 2001]. The origin of the AMO is not fully understood; however, various research has suggested that it may be related to the meridional overturning circulation of the Atlantic Ocean (AMOC; aka the Atlantic thermohaline circulation) [*Delworth and Mann*, 2000; *Knight et al.*, 2005], the regional air-sea interaction, or adjacent land/ice process [*Cheng et al.*, 2004; *Dima and Lohmann*, 2007]. The impact that the AMO/AMOC has on the climate reaches the adjacent areas as well as the eastern tropical Pacific region. *Dong et al.* [2006] argued that the Atlantic sea surface temperature (SST) that correlates to a positive AMO reduces El Niño–Southern Oscillation (ENSO) variability, mainly through atmospheric teleconnection, which is the atmospheric bridge from the Atlantic Ocean to the Pacific Ocean. This results in relaxed trade winds, which lead to a deepening of the thermocline and a reduction of the vertical stratification in the equatorial Pacific Ocean, which suppresses the ENSO. Conversely, *Timmermann et al.* [2005] argued that the weakening of the AMOC, caused by a positive freshwater flux into the Atlantic Ocean, leads to a deepening of the zonal mean tropical Pacific thermocline through a readjustment of the global thermocline (so-called "seiching mechanism"), which in turn suppresses ENSO variability. In subsequent research, *Timmermann et al.* [2007] argued that the weakening of the AMOC (i.e., negative phase of the AMO) leads to a weakening of the annual cycle in the equatorial Pacific, which strengthens ENSO variability through nonlinear interaction (comprising a so-called "frequency-entrainment" mechanism).

In this research, we propose another process, emphasizing the changes in the atmosphere-ocean coupling strength corresponding to the mean tropical Pacific SST changes associated with the AMO. In particular, since the atmospheric circulation over the tropics is mainly driven by deep convection, the relationship between deep convection and SST is crucial to ENSO variability. In this study, we examined the nonlinear relationship between SST and atmospheric convection related to changes in the background SST, determining the influence of the AMO. While previous studies highlighting the impact of the AMO/AMOC on the ENSO have been predominantly based on numerical model experiments, in this research we analyze mainly the observed data, although the sampling size is limited, which enables us to identify processes in the model that has previously been overlooked due to model biases. In addition, we analyzed a long-term climate model simulation to better critique our observational findings.

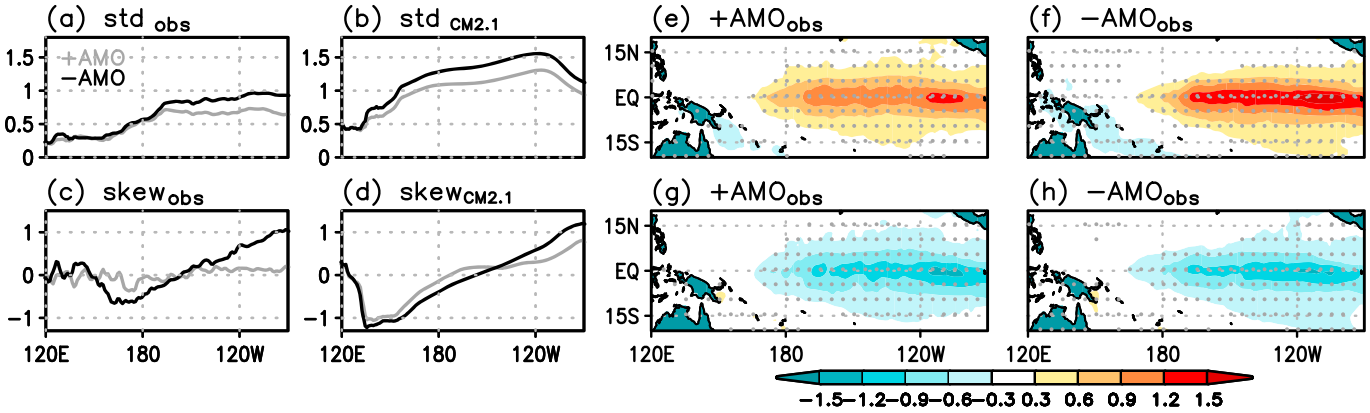

Figure 1. Standard deviation of equatorial (5°S–5°N) SST anomalies with respect to AMO phase (grey: +AMO, black: −AMO) in (a) HadISST and (b) CM2.1. (c and d) The same as Figures 1a and 1b, except for skewness of SST. (e and f) A composite of HadISST anomalies during October to December for El Niño years that belong to +AMO and −AMO periods, respectively (in °C). Prior to composite analysis, the mean SST covariant with the AMO was removed from the SST anomaly. (g and h) The same as Figures 1e and 1f , except for La Niña years (El Niño: 10 (+AMO) and 22 (−AMO) years, La Niña: 15 (+AMO) and 20 (−AMO) years). Stippled areas indicate significant anomalies at the 95% confidence level based on a *t* test.

2. Data and Methods

We analyzed both the observational data and a long-term simulation output in order to understand the oceanic and atmospheric variability associated with the AMO. The observational SST data were obtained from the Met Office Hadley Centre [*Rayner et al.*, 2003]. Following the definition given by *Trenberth and Shea* [2006], the AMO index was calculated based on the annual SST anomalies for the North Atlantic (0–60°N, 0–80°W), smoothed by the 10 year running mean. This AMO index coincides with other indices from previous research, with the exception of the period prior to 1900 [*Knight et al.*, 2005; *Trenberth and Shea*, 2006]. Due to this lack of historical data, in this research we focused on the period from 1900 to 2012, which includes a positive AMO (+AMO) for 48 years (1927–1964 and 1999–2008) and a negative AMO (−AMO) for a period of 61 years (1900–1926 and 1965–1998). Linear trends in the Hadley Centre Global Sea Ice and Sea Surface Temperature (HadISST) data were removed for the analysis period, and the selected ENSO years had the criterion that the Niño 3 index (SST anomalies averaged over 5°S–5°N, 90–150°W) from October to December was above or below ±0.5 standard deviation.

The Global Precipitation Climatology Project (GPCP) monthly precipitation data were obtained from the National Oceanic and Atmospheric Administration website at http://www.esrl.noaa.gov/psd/ [*Adler et al.*, 2003]. The GPCP data begin with the year 1979. We also used atmospheric reanalysis data from the National Center for Environmental Prediction/National Center for Atmospheric Research, which dates back to 1948 [*Kalnay et al.*, 1996].

Because the available observations are rather short to deal with the multidecadal timescale phenomenon, we also analyzed a 500 year output from the Geophysical Fluid Dynamics Laboratory CM2.1 coupled model. The model output, known as a "preindustrial control experiment" with a fixed atmospheric carbon composition based on the data for the year 1860, was downloaded from the Program for Climate Model Diagnosis and Intercomparison archive [*Delworth et al.*, 2006; *Wittenberg et al.*, 2006]. These data cover 270 + AMO years and 221 − AMO years. In order to evaluate the difference between the +AMO and −AMO periods, we performed a Monte Carlo test using 1000 random sample groups with the same sizes as the two AMO periods.

3. Results

As previously mentioned, −AMO is known to promote ENSO variability by modulating the mean state in the eastern tropical Pacific [*Dong et al.*, 2006; *Timmermann et al.*, 2007]. Specifically, the monthly standard deviation of Niño 3 SST increased 22% during the cold phase of the AMO compared to the warm phase [*Dong et al.*, 2006]. The standard deviation of equatorial SST anomalies over the eastern Pacific increased during −AMO periods (Figures 1a and 1b). For the Niño 3 region, the standard deviation of the monthly

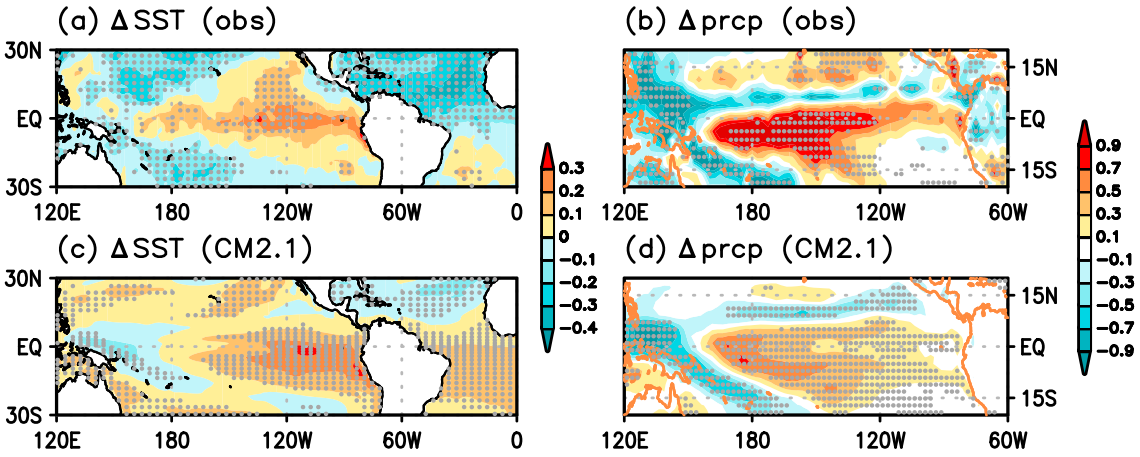

Figure 2. Differences of annual mean of (a) HadISST (°C) and (b) GPCP precipitation (mm/day) between negative and positive AMO periods. (c and d) The same as Figures 2a and 2b except for using CM2.1 simulation output. Stippled areas indicate a significant difference at 90% and 95% confidence levels for observation and CM2.1, respectively.

SST anomalies increased by 31% and 21% during the −AMO periods compared to those of +AMO period from the observational data and the model, respectively.

It is interesting to note that there were distinct differences in the intensification of El Niño and La Niña events. The SST anomalies in the El Niño years during −AMO periods were stronger; however, the intensity of La Niña events for −AMO years were comparable to those with +AMO periods (Figures 1e–1h). Prior to this analysis, we removed the mean SST covariant with the AMO from the SST anomaly. As a −AMO period tends to accompany warmer mean SST conditions over the central-to-eastern equatorial Pacific, as shown in Figures 2a and 2c [*Hong et al.*, 2013; *Koutavas et al.*, 2002; *Stott et al.*, 2002; *Sutton and Hodson*, 2007], the mean state exhibits seasonal variation. In order to remove the seasonally varying mean SST difference associated with AMO from the anomalies, we first calculated the linear regression coefficient of the SST with respect to the AMO index for each calendar month. We subsequently subtracted the regression coefficient from the SST anomaly after weighting it using the AMO index. Therefore, the differences in the SST anomalies in Figure 1 indicate the interannual differences of the ENSO variability, in which warmer mean states induced by −AMO are excluded.

The asymmetrical enhancement between El Niño and La Niña events is also seen more clearly in the skewness patterns (Figures 1c and 1d), such that the SST anomalies are more positively skewed over the eastern tropical Pacific during −AMO periods. The positive skewness of the eastern tropical Pacific SST indicates that a stronger development of an El Niño event, compared to a La Niña event, is more likely during −AMO periods. The coherent features are also shown in CM2.1. It indicates that the asymmetric enhancement of El Niño-La Niña events during −AMO periods was not a sampling problem; rather, there was a physical process supporting this phenomenon. The asymmetric impact of the AMO on El Niño and La Niña events also suggests that the underlying physical processes are not linear.

Although we disregarded the mean state difference over the equatorial Pacific in association with the AMO for our initial analysis, we assumed that changes in the residual mean state were still responsible for the asymmetric development of the ENSO, since the tropical ocean-atmosphere mean state is a key factor controlling El Niño characteristics [e.g., *An and Wang*, 2000; *Fedorov and Philander*, 2001]. Figures 2b and 2d show the changes in the precipitation during the −AMO periods. Precipitation increases along the equator, which is in contrast to the suppressed precipitation that occurs to the north of the enhanced precipitation region commonly seen in the observations and model output. These features are consistent with a southward shift of the Intertropical Convergence Zone (ITCZ) during −AMO periods, which was identified in earlier studies [*Dong et al.*, 2006; *Zhang and Delworth*, 2005]. Changes in various physical mean variables are closely linked to each other. Climatologically, the eastern tropical Pacific region is characterized by cold surface temperatures, owing to equatorial upwelling. The cold SST in the mean state suppresses atmospheric convection and forces the maximum convection region (i.e., ITCZ) away from the

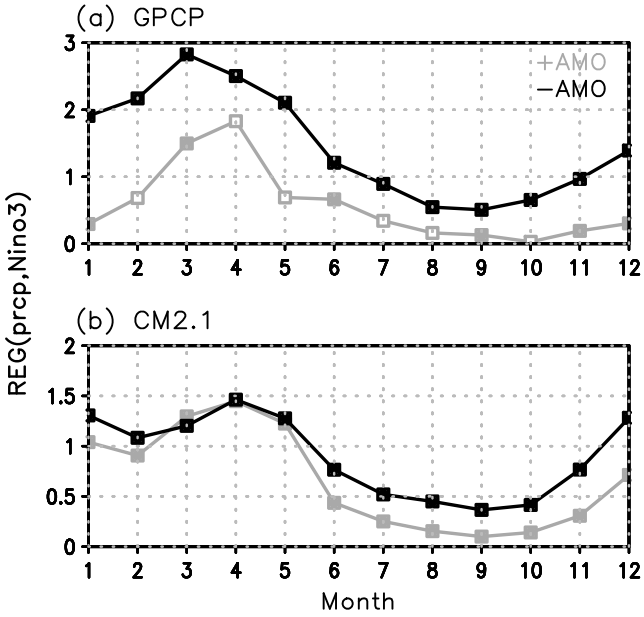

Figure 3. (a) Regression coefficients of precipitation over the eastern tropical Pacific against the Niño 3 SST for each calendar month for the periods of +AMO (gray) and −AMO (black) in the observation. (b) Same as Figure 3a except for CM2.1 output. Units are mm day^{-1} °C^{-1}. Closed squares indicate significant coefficients at 95% confidence level on a *t* test.

equator [*Li*, 1997; *Xie and Philander*, 1994]. Therefore, the warmer mean state in the eastern Pacific, due to −AMO periods, can pull the climatological location of the ITCZ south, closer to the equator. The warmer mean state has important implications, not only for the climatological distribution of convection but also for the interannual development of ENSO. We also examined the nonlinear response of atmospheric convection in El Niño and La Niña events with respect to underlying SST changes, which leads to uneven growth for the ENSO. Previous studies determined that atmospheric convection is significantly correlated with collocated SST in the eastern tropical Pacific region [*Gutzler and Wood*, 1990; *Lau et al.*, 1997] and that atmospheric convection increases exponentially, rather than linearly, as the SST increases (see Figure S1 in the supporting information). For example, the increased amount of precipitation for the 26–27°C SST range is distinctly larger than that for the range below 26°C and the increased amount of precipitation for the higher SST range is even larger. This nonlinear relationship between SST and precipitation implies that the atmospheric response to the same SST anomaly can differ according to total SST. This relationship between SST and precipitation does not change much with changes in the AMO phase (not shown).

The effect of precipitation on the SST magnitude indicates that there is a different atmospheric sensitivity for the various basic states of the ocean. Warmer mean surface conditions over the central-to-eastern equatorial Pacific enhance atmospheric sensitivity during −AMO periods. In order to assess the influence of changes in the ocean's mean state on the ENSO, we first calculated the regression coefficients of the Niño 3 region for the average precipitation amounts, with respect to the Niño 3 SST anomalies for each calendar month during the AMO phases (Figure 3). These results enabled us to compare the atmospheric sensitivity to the unit SST forcing for the +AMO and −AMO periods. In both the observation and model outputs, the regression coefficients exhibited larger overall values during −AMO periods, especially for the months from June to November. The larger regression coefficients during −AMO periods indicate increased precipitation for the same SST anomalies, implying increased atmospheric sensitivity. The increased atmospheric sensitivity in these seasons is important for ENSO intensity, because these seasons are regarded as comprising an ENSO growing phase. The aforementioned results verify that the atmospheric responses to the SST anomalies are enhanced during −AMO periods; however, this does not mean that it works more favorably for warm phases of the ENSO. Therefore, in order to assess the difference in the atmospheric sensitivity to SST anomalies between El Niño and La Niña events for each AMO phase, we further computed the air-sea coupling strength, which is defined as the linear regression coefficients of the monthly zonal wind stress anomalies with respect to the Niño 3 index (Figure 4). For a comparison between El Niño and La Niña events, the regression coefficients were calculated only for years in which El Niño and La Niña events occurred. We identified 7 and 10 (11 and 13) El Niño (La Niña) events for the +AMO and −AMO periods, respectively. For the model output, we applied the same criteria used in the observational data, and 58 and 58 (82 and 71) El Niño (La Niña) events are obtained for the +AMO and −AMO periods, respectively.

As seen in Figure 4, the positive peaks of the zonal wind stress anomalies were found over the central Pacific, in both the observational and model data, implying a strong air-sea coupling between wind stress and Niño 3

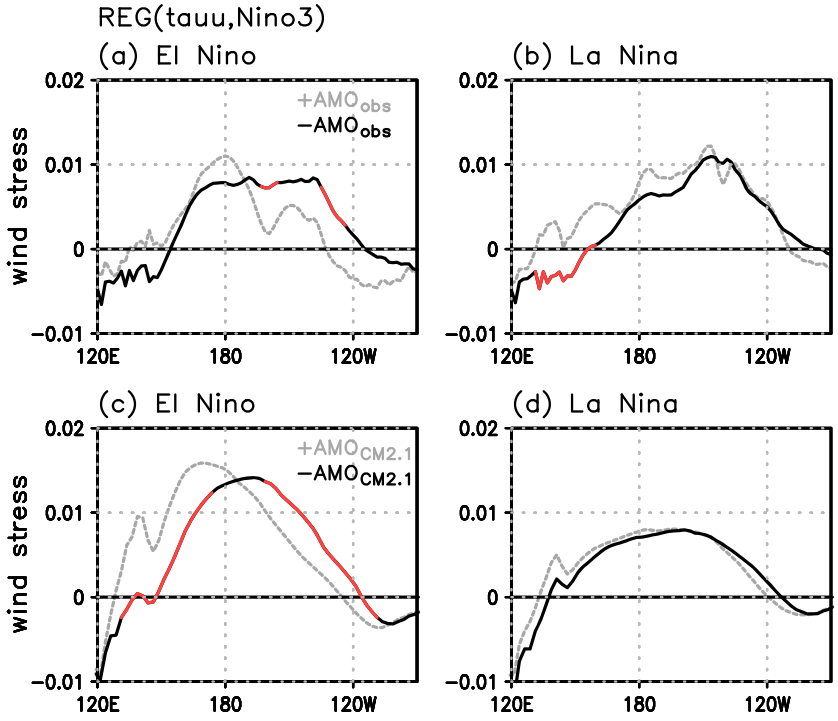

Figure 4. Equatorially averaged (5°S–5°N) linear regression coefficient of monthly zonal wind stress anomaly with respect to the monthly Niño 3 index for January to December of (a) El Niño and (b) La Niña developing years that belong to positive (grey solid line) and negative (black dashed line) AMO periods in the observation. (c and d) The same as Figures 4a and 4b except for CM2.1. The regions of significant differences at 90% and 95% confidence level are indicated by red for observation and CM2.1 output, respectively.

SST. During the El Niño years (Figure 4a), the peak extended farther eastward during −AMO periods, which is consistent with the increased atmospheric sensitivity during −AMO periods, as inferred by the precipitation anomalies shown in Figure 3. As wind stress moved eastward, the SST anomalies over the equatorial Pacific became stronger, and the duration of the ENSO episodes also lengthened [*An and Wang*, 2000; *Kang and Kug*, 2002]. This is because the delayed negative feedback from the oceanic Rossby waves had more of a lag, which allowed the El Niño event to have more time to grow. The CM2.1 model reproduced the characteristics of wind stress anomaly over the central and eastern Pacific during −AMO periods (Figure 4c). For the La Niña years, the zonal wind stress anomalies did not show a meaningful contrast between the +AMO and −AMO periods (Figures 4b and 4d). In addition, the intensity of the wind stress anomalies was nearly the same between +AMO and −AMO periods, with similar features being also found in their zonal structures. As a result, the asymmetric atmospheric responses to El Niño and La Niña events confirm the asymmetric impact of different AMO phases on the air-sea coupling strength, which can be attributed to the nonlinearity of the convection-SST relationship.

4. Summary and Discussion

ENSO activity tends to be amplified when the North Atlantic is under a cold mean state [*Dong et al.*, 2006; *Timmermann et al.*, 2007]. In this study, using both observational data and a Coupled General Circulation Model (CGCM) output, we examined the changes in the ENSO characteristics according to the AMO phase and found that El Niño events were more significantly enhanced than La Niña events during −AMO periods. The asymmetric development of the ENSO during the different AMO phases is related to the warmer and wetter basic state of the central-to-eastern tropical Pacific, as shown in both the observations and the CM2.1 model output. Owing to the nonlinear properties in the SST-convection relationship, the warmer mean state of the SST in the central-to-eastern tropical Pacific enhances the sensitivity of atmospheric convection to the same SST anomaly; consequently, this strengthens the atmosphere-ocean

coupled feedback processes. The enhanced air-sea coupling strength during −AMO periods is more favorable to the development of El Niño events than La Niña events. In particular, there is an eastward shift of atmospheric responses to SST anomalies during El Niño growing seasons.

Up to now, as seen in the other numerical modeling studies, the tropical Pacific response to changes in Atlantic circulation was quite diverse [*Cessi et al.*, 2004; *Dong et al.*, 2006; *Knight et al.*, 2005; *Timmermann et al.*, 2007]. In fact, the model output in this study also showed that the La Niña amplitude during −AMO increases as much as El Niño amplitude, which is different from the observed. These inconsistencies with the observation or between models may be attributed to the model bias, in particular, an overly developed cold SST anomaly over the equatorial eastern Pacific. As emphasized in this study, the total SST over the eastern Pacific is more important than SST anomalies in driving atmospheric convection. Perhaps, the simulated colder mean tropical eastern Pacific SST may be far below than a threshold of total SST for emergence of the nonlinear relationship between SST anomaly and atmospheric convection. Thus, the impact due to the nonlinear SST-convection relationship may be missed in most models, and it results in a weaker El Niño-La Niña asymmetry under different AMO condition. To verify this point, however, a further analysis needs to be pursued that might be beyond the current scope.

Several studies have emphasized the importance of a warm and wet eastern Pacific basic state on ENSO characteristics. For example, *Kim et al.* [2011] argued that the east-west contract in the tropical Pacific mean SST is crucial for ENSO variability. They found that when the east-west SST contrast is reduced, the mean precipitation over the eastern Pacific increases, and the atmospheric responses to the SST anomalies are shifted eastward. Therefore, effective atmospheric feedback leads to intensified ENSO variability. The climatic impact of a reduced east-west contrast in the equatorial Pacific seems to correspond to a weakened mean zonal circulation (i.e., the Walker circulation). As the Walker circulation weakens, the subsidence in the descending branch of Walker circulation promotes more frequent triggering of convection. The increased probability of the development of atmospheric convection over the eastern tropical Pacific region facilitates an eastward shift for atmospheric responses. Therefore, the stronger growth of El Niño events during −AMO periods is partially attributed to such an effect, since the warmer mean SST over the eastern tropical Pacific reduces the east-west SST contrast. In this study, we attributed the stronger development of El Niño events during −AMO periods to the warmer SST itself. Atmospheric convection strength is governed by the moist static energy of air parcels, which depends on the SST itself. Therefore, it is arguable that both an increased mean SST over the eastern Pacific and a reduced east-west contrast collectively contribute to the strong development of El Niño events during −AMO periods. For a better understanding of the two processes and how they relate to one another, more in-depth research is needed.

Acknowledgments

We acknowledge the World Climate Research Programme's Working Group on Coupled Modelling, which is responsible for CMIP, and we thank the climate modeling groups for producing and making available their model output at http://pcmdi9.llnl.gov/. For CMIP, the U.S. Department of Energy's Program for Climate Model Diagnosis and Intercomparison provides coordinating support and led development of software infrastructure in partnership with the Global Organization for Earth System Science Portals. M.K. Sung and B.M. Kim are supported by Korea Polar Research Institute (PE15010), and S.I. An is supported by the National Research Foundation of Korea grant funded by the Korean Government (MEST) (NRF-2009-0093069).

The Editor thanks two anonymous reviewers for their assistance in evaluating this paper.

References

Adler, R. F., G. J. Huffman, A. Chang, R. Ferraro, P.-P. Xie, J. Janowiak, B. Rudolf, U. Schneider, S. Curtis, and D. Bolvin (2003), The version-2 Global Precipitation Climatology Project (GPCP) monthly precipitation analysis (1979–present), *J. Hydrometeorolm.*, *4*(6).

An, S.-I., and B. Wang (2000), Interdecadal change of the structure of the ENSO mode and its impact on the ENSO frequency*, *J. Clim.*, *13*(12), 2044–2055.

Cessi, P., K. Bryan, and R. Zhang (2004), Global seiching of thermoclime waters between the Atlantic and the Indian-Pacific Ocean Basins, *Geophys. Res. Lett.*, *31*, L04302, doi:10.1029/2003GL019091.

Cheng, W., R. Bleck, and C. Rooth (2004), Multi-decadal thermohaline variability in an ocean-atmosphere general circulation model, *Clim. Dyn.*, *22*(6–7), 573–590.

Delworth, T. L., and M. E. Mann (2000), Observed and simulated multidecadal variability in the Northern Hemisphere, *Clim. Dyn.*, *16*(9), 661–676.

Delworth, T. L., et al. (2006), GFDL's CM2 global coupled climate models. Part I: Formation and simulation characteristics, *J. Clim.*, *19*, 634–674.

Dima, M., and G. Lohmann (2007), A hemispheric mechanism for the Atlantic multidecadal oscillation, *J. Clim.*, *20*, 2706–2719.

Dong, B., R. T. Sutton, and A. A. Scaife (2006), Multidecadal modulation of El Niño-Southern Oscillation (ENSO) variance by Atlantic Ocean sea surface temperatures, *Geophys. Res. Lett.*, *33*, L08705, doi:10.1029/2006GL025766.

Enfield, D. B., A. M. Mestas-Nuñez, and P. J. Trimble (2001), The Atlantic multidecadal oscillation and its relation to rainfall and river flows in the continental US, *Geophys. Res. Lett.*, *28*(10), 2077–2080, doi:10.1029/2000GL012745.

Fedorov, A. V., and S. G. Philander (2001), A stability analysis of tropical ocean-atmosphere interactions: Bridging measurements and theory for El Niño, *J. Clim.*, *14*(14), 3086–3101.

Gutzler, D. S., and T. M. Wood (1990), Structure of large-scale convective anomalies over tropical oceans, *J. Clim.*, *3*(4), 483–496.

Hong, S., I.-S. Kang, I.-D. Choi, and Y.-G. Ham (2013), Climate responses in the tropical Pacific associated with Atlantic warming in recent decades, *Asia Pacific J. Atmos. Sci.*, *49*(2), 209–217.

Kalnay, E., M. Kanamitsu, R. Kistler, W. Collins, D. Deaven, L. Gandin, M. Iredell, S. Saha, G. White, and J. Woollen (1996), The NCEP/NCAR reanalysis project, *Bull. Am. Meteorol. Soc.*, *77*(3), 437–471.

Kang, I.-S., and J.-S. Kug (2002), El Niño and La Niña sea surface temperature anomalies: Asymmetry characteristics associated with their wind stress anomalies, *J. Geophys. Res.*, *107*(D19), 4372, doi:10.1029/2001JD000393.
Kerr, R. A. (2000), A North Atlantic climate pacemaker for the centuries, *Science*, *288*(5473), 1984–1985.
Kim, D., Y. S. Jang, D. H. Kim, Y. H. Kim, M. Watanabe, F.-F. Jin, and J.-S. Kug (2011), El Niño-Southern Oscillation sensitivity to cumulus entrainment in a coupled general circulation model, *J. Geophys. Res.*, *116*, D22112, doi:10.1029/2011JD016526.
Knight, J. R., R. J. Allan, C. K. Folland, M. Vellinga, and M. E. Mann (2005), A signature of persistent natural thermohaline circulation cycles in observed climate, *Geophys. Res. Lett.*, *32*, L20708, doi:10.1029/2005GL024233.
Koutavas, A., J. Lynch-Stieglitz, T. M. Marchitto, and J. P. Sachs (2002), El Niño-like pattern in ice age tropical Pacific sea surface temperature, *Science*, *297*(5579), 226–230.
Lau, K. M., H. T. Wu, and S. Bony (1997), The role of large-scale atmospheric circulation in the relationship between tropical convection and sea surface temperature, *J. Clim.*, *10*(3), 381–392.
Li, T. (1997), Air-sea interactions of relevance to the ITCZ: Analysis of coupled instabilities and experiments in a hybrid coupled GCM, *J. Atmos. Sci.*, *54*(1), 134–147.
Rayner, N. A., D. E. Parker, E. B. Horton, C. K. Folland, L. V. Alexander, D. P. Rowell, E. C. Kent, and A. Kaplan (2003), Global analyses of sea surface temperature, sea ice, and night marine air temperature since the late nineteenth century, *J. Geophys. Res.*, *108*(D14), 4407, doi:10.1029/2002JD002670
Schlesinger, M. E., and N. Ramankutty (1994), An oscillation in the global climate system of period 65–70 years, *Nature*, *367*(6465), 723–726.
Stott, L., C. Poulsen, S. Lund, and R. Thunell (2002), Super ENSO and global climate oscillations at millennial time scales, *Science*, *297*(5579), 222–226.
Sutton, R. T., and D. L. R. Hodson (2007), Climate response to basin-scale warming and cooling of the North Atlantic Ocean, *J. Clim.*, *20*(5), 891–907.
Timmermann, A., S.-I. An, U. Krebs, and H. Goosse (2005), ENSO suppression due to weakening of the North Atlantic thermohaline circulation, *J. Clim.*, *18*(16).
Timmermann, A., Y. Okumura, S.-I. An, A. Clement, B. Dong, E. Guilyardi, A. Hu, J. H. Jungclaus, M. Renold, and T. F. Stocker (2007), The influence of a weakening of the Atlantic meridional overturning circulation on ENSO, *J. Clim.*, *20*(19).
Trenberth, K. E., and D. J. Shea (2006), Atlantic hurricanes and natural variability in 2005, *Geophys. Res. Lett.*, *33*, L12704, doi:10.1029/2006GL026894.
Wittenberg, A. T., A. Rosati, N. C. Lau, and J. J. Ploshay (2006), GFDL's CM2 global coupled climate models. Part III: Tropical Pacific climate and ENSO, *J. Clim.*, *19*, 698–722.
Xie, S. P., and S. G. H. Philander (1994), A coupled ocean-atmosphere model of relevance to the ITCZ in the eastern Pacific, *Tellus A*, *46*(4), 340–350.
Zhang, R., and T. L. Delworth (2005), Simulated tropical response to a substantial weakening of the Atlantic thermohaline circulation, *J. Clim.*, *18*(12).